

# Self-trapping of the $d$ - $d$ charge transfer exciton in bulk NiO evidenced by $X$ -ray excited luminescence

V. I. Sokolov, V. A. Pustovarov<sup>+</sup>, V. N. Churmanov<sup>+</sup>, V. Yu. Ivanov<sup>+</sup>, N. B. Gruzdev, P. S. Sokolov\*, A. N. Baranov\*, A. S. Moskvina<sup>×1)</sup>

*Institute of Metal Physics UD RAS, 620990 Ekaterinburg, Russia*

<sup>+</sup>*Ural Federal University, 620002 Ekaterinburg, Russia*

<sup>\*</sup>*Lomonosov Moscow State University, 119991 Moscow, Russia*

<sup>×</sup>*Department of Theoretical Physics, Institute of Natural Science, Ural Federal University, 620083 Ekaterinburg, Russia*

Submitted 4 April 2012

Soft  $X$ -ray (XUV) excitation did make it possible to avoid the predominant role of the surface effects in luminescence of NiO and revealed a bulk luminescence with a puzzling well isolated doublet of very narrow lines with close energies near 3.3 eV which is assigned to recombination transitions in self-trapped  $d$ - $d$  charge transfer (CT) excitons formed by coupled Jahn–Teller  $Ni^+$  and  $Ni^{3+}$  centers. The conclusion is supported both by a comparative analysis of the CT luminescence spectra for NiO and solid solutions  $Ni_xZn_{1-x}O$ , and by a comprehensive cluster model assignment of different  $p$ - $d$  and  $d$ - $d$  CT transitions, their relaxation channels. To the best of our knowledge it is the first observation of the luminescence due to self-trapped  $d$ - $d$  CT excitons.

**Introduction.** Charge carriers and excitons photo-generated in a crystal with strong electron-lattice interaction are known to relax to self-trapped states causing local lattice deformation and forming luminescence centers [1]. Some quite basic questions concerning the self-trapped exciton remain unresolved, even in the alkali halides which are traditionally regarded as prototype insulating materials in which the microscopic features of the self-trapping processes have been studied most extensively. The situation seems to be more obscure for transition metal compounds, in particular, for self-trapping of the  $p$ - $d$  and  $d$ - $d$  charge transfer (CT) excitons. The  $p$ - $d$  CT excitons have been observed in II–VI: $3d$  compounds as narrow lines preceding broad intensive  $p$ - $d$  CT absorption bands [2]. Most likely, the CT excitons have not been observed in photoluminescence mainly due to nonradiative transitions to intra-center  $3d$  states, hence the  $d$ - $d$  crystal field transitions are usually the main contributors to photoluminescence of  $3d$  compounds. Observation of green luminescence in ZnO:Cu with a sharp zero-phonon line at 2.859 eV is perhaps the only reliable evidence of the self-trapping and radiative deexcitation of the  $p$ - $d$  CT exciton [3]. Uniqueness of ZnO:Cu is that the radiative  $p$ - $d$  CT transition is well isolated from the only crystal field  $3d^9: {}^2E \rightarrow 3d^9: {}^2T_2$  transition by the energy gap of almost 2 eV that blocks the non-radiative deexcitation of the CT state. Interestingly, that a similar situation with observation of

the ligand-cation CT luminescence is realized in a large body of compounds with rare-earth  $Yb^{3+}$  ion [4]. To the best of our knowledge, there is no reliable literature data regarding the observation of the self-trapping for  $d$ - $d$  CT excitons. Apparently the appearance of the unconventional  $d$ - $d$  CT luminescence is feasible only under specific conditions. Here we would like to point to  $d$ - $d$  CT exciton formed by the electron/hole transfer in  $Ni^{2+}$ – $Ni^{2+}$  pairs in nickel monoxide NiO to be a unique candidate for the self-trapping accompanied by  $d$ - $d$  CT luminescence. In NiO one expects a strong  $d$ - $d$  CT transition related with the  $\sigma$ – $\sigma$ -type  $e_g$ – $e_g$  charge transfer  $t_{2g}^6 e_g^2 + t_{2g}^6 e_g^2 \rightarrow t_{2g}^6 e_g^3 + t_{2g}^6 e_g^1$  between  $nnn$  Ni sites with the creation of electron  $[NiO_6]^{11-}$  and hole  $[NiO_6]^{9-}$  centers (electron-hole dimer), or nominally  $Ni^+$  and  $Ni^{3+}$  ions. This unique anti-Jahn–Teller transition  ${}^3A_{2g} + {}^3A_{2g} \rightarrow {}^2E_g + {}^2E_g$  creates a  $d$ - $d$  CT exciton prone to be self-trapped in the lattice due to electron-hole attraction and strong “double” Jahn–Teller effect for the both electron and hole centers. Below, in the Letter we present a comprehensive cluster model description of the  $p$ - $d$  and  $d$ - $d$  CT transitions in NiO and experimental results of the measurements of the  $X$ -ray excited luminescence which evidence the manifestation of the  $d$ - $d$  CT luminescence.

**$p$ - $d$  and  $d$ - $d$  CT transitions in NiO.** Explaining the electronic properties of transition metal monoxides is one of the long-standing problems in the condensed matter physics. Nickel monoxide NiO with its rather simple rocksalt structure, a large insulating gap and an

<sup>1)</sup> e-mail: alexandr.moskvina@usu.ru

antiferromagnetic ordering temperature of  $T_N = 523$  K has been attracting many physicists as a prototype oxide for this problem. This strongly correlated electron material has played and is playing a very important role in clarifying the electronic structure and understanding the rich physical properties of 3d compounds. Despite several decades of studies [5] there is still no literature consensus on the detailed electronic structure of NiO and comprehensive assignment of different spectral features. However, some reliable semiquantitative predictions can be made in frames of a simple cluster approach (see, e.g. Refs. [6] and references therein). The method provides a clear physical picture of the complex electronic structure and the energy spectrum, as well as the possibility of a quantitative modelling. In a certain sense the cluster calculations might provide a better description of the overall electronic structure of insulating 3d oxides than the band structure calculations, mainly due to a better account for correlation effects. Starting with octahedral  $\text{NiO}_6$  complex with the point symmetry group  $O_h$  we deal with five Ni 3d and eighteen oxygen O 2p atomic orbitals forming both hybrid Ni 3d-O 2p bonding and antibonding  $e_g$  and  $t_{2g}$  molecular orbitals (MO), and purely oxygen nonbonding  $a_{1g}(\sigma)$ ,  $t_{1g}(\pi)$ ,  $t_{1u}(\sigma)$ ,  $t_{1u}(\pi)$ ,  $t_{2u}(\pi)$  orbitals. Ground state of  $[\text{NiO}_6]^{10-}$  cluster, or nominally  $\text{Ni}^{2+}$  ion corresponds to  $t_{2g}^6 e_g^2$  configuration with the Hund  ${}^3A_{2g}$  ground term. Typically for the octahedral  $\text{MeO}_6$  clusters [6] the non-bonding  $t_{1g}(\pi)$  oxygen orbital has the highest energy and forms the first electron removal oxygen state while other nonbonding oxygen  $\pi$ -orbitals,  $t_{2u}(\pi)$ ,  $t_{1u}(\pi)$ , and  $\sigma$ -orbital  $t_{1u}(\sigma)$  have lower energy with the energy separation  $\sim 1$  eV in between (see Fig. 1).

The  $p$ - $d$  CT transition in  $\text{NiO}_6^{10-}$  center is related with the transfer of O 2p electron to the partially filled  $3d e_g$ -subshell with formation on the Ni-site of the  $(t_{2g}^6 e_g^3)$  configuration of nominal  $\text{Ni}^+$  ion isoelectronic to the well-known Jahn-Teller  $\text{Cu}^{2+}$  ion. Yet actually instead of a single  $p$ - $d$  CT transition we arrive at a series of O  $2p\gamma \rightarrow \text{Ni } 3d e_g$  CT transitions forming a complex  $p$ - $d$  CT band. It should be noted that each single electron  $\gamma \rightarrow e_g$   $p$ - $d$  CT transition starting with oxygen  $\gamma$ -orbital gives rise to several many-electron CT states. For  $\gamma = t_{1,2}$  these are singlet and triplet terms  ${}^1, {}^3T_{1,2}$  for configurations  $t_{2g}^6 e_g^3 t_{1,2}$ , where  $t_{1,2}$  denotes the oxygen hole.

The complex  $p$ - $d$  CT band starts with the dipole-forbidden  $t_{1g}(\pi) \rightarrow e_g$ , or  ${}^3A_{2g} \rightarrow {}^1, {}^3T_{1g}, {}^1, {}^3T_{2g}$  transitions, then includes two formally dipole-allowed so-called  $\pi \rightarrow \sigma$   $p$ - $d$  CT transitions, weak  $t_{2u}(\pi) \rightarrow e_g$ , and relatively strong  $t_{1u}(\pi) \rightarrow e_g$  CT transitions, respectively, each giving rise to  ${}^3A_{2g} \rightarrow {}^3T_{2u}$  transitions. Finally

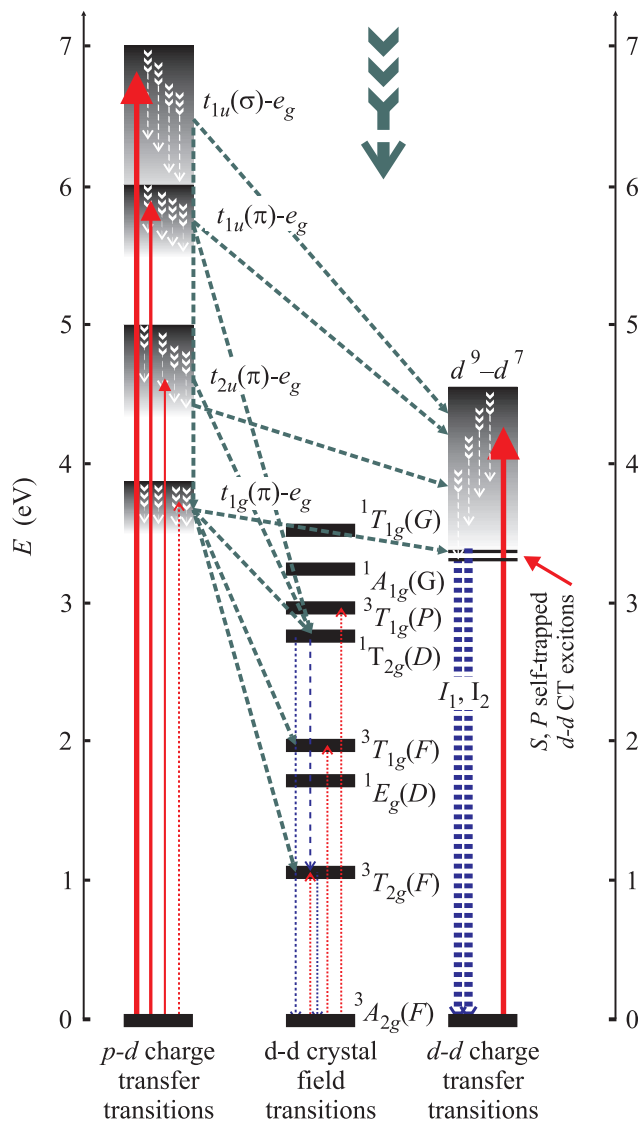


Fig. 1. (Color online) Spectra of the  $d$ - $d$ ,  $p$ - $d$  CT transitions and intracenter crystal field  $d$ - $d$  transitions in NiO. Strong dipole-allowed  $\sigma$ - $\sigma$ -type,  $d$ - $d$ , and  $p$ - $d$  transitions are shown by thick solid arrows; weak dipole-allowed  $\pi$ - $\sigma$ ,  $p$ - $d$  transitions by thin solid arrows; weak dipole-forbidden low-energy transitions by thin dashed arrows, respectively. Dashed lines point to different electron-hole relaxation channels, dotted lines point to PL transitions. Spectrum of the crystal field transitions is reproduced from Ref. [7]

main  $p$ - $d$  CT band is ended by the strongest dipole-allowed  $\sigma \rightarrow \sigma$   $t_{1u}(\sigma) \rightarrow e_g$  ( ${}^3A_{2g} \rightarrow {}^3T_{2u}$ ) CT transition. Above estimates predict the separation between partial  $p$ - $d$  bands to be  $\sim 1$  eV. Thus, if the most intensive CT band with a maximum around 7 eV observed in RIXS spectra [8, 9] to attribute to the strongest dipole-allowed O  $2p t_{1u}(\sigma) \rightarrow \text{Ni } 3d e_g$  CT transition then one should expect the low-energy  $p$ - $d$  CT counterparts with

maximума around 4, 5, and 6 eV respectively, which are related to dipole-forbidden  $t_{1g}(\pi) \rightarrow e_g$ , weak dipole-allowed  $t_{2u}(\pi) \rightarrow e_g$ , and relatively strong dipole-allowed  $t_{1u}(\pi) \rightarrow e_g$  CT transitions, respectively (see Fig. 1). It is worth noting that the  $\pi \rightarrow \sigma$   $p$ - $d$  CT  $t_{1u}(\pi) - e_g$  transition borrows a portion of intensity from the strongest dipole-allowed  $\sigma \rightarrow \sigma$   $t_{1u}(\sigma) \rightarrow e_g$  CT transition because the  $t_{1u}(\pi)$  and  $t_{1u}(\sigma)$  states of the same symmetry are partly hybridized due to  $p$ - $p$  covalency and overlap. Interestingly that this assignment finds a strong support in the reflectance (4.9, 6.1, and 7.2 eV for allowed  $p$ - $d$  CT transitions) spectra of NiO [10]. A rather strong  $p(\pi)$ - $d$  CT band peaked at 6.3 eV is clearly visible in the absorption spectra of MgO:Ni [11]. Electroreflectance spectra [12] which detect dipole-forbidden transitions clearly point to a low-energy forbidden transition peaked near 3.7 eV missed in reflectance and absorption spectra [7, 10, 11], which thus defines a  $p$ - $d$  character of the optical CT gap and can be related with the onset transition for the whole complex  $p$ - $d$  CT band. It should be noted that a peak near 3.8 eV has been also observed in nonlinear absorption spectra of NiO [13]. At variance with the bulk NiO a clearly visible intensive CT peak near 3.6–3.7 eV has been observed in absorption spectra of NiO nanoparticles [14, 15]. This strongly supports the conclusion that the 3.7 eV band is related with the bulk-forbidden CT transition which becomes the allowed one in the nanocrystalline state. It is worth noting that the hole-type photoconductivity threshold in bulk NiO has been observed also at this “magic” energy 3.7 eV [16], that is the  $t_{1g}(\pi) \rightarrow e_g$   $p$ - $d$  CT transition is believed to produce itinerant holes. Indeed, as a result of the  $p$ - $d$  CT transition, a photo-generated electron localizes on a  $\text{Ni}^{2+}$  ion forming Jahn–Teller  $3d^9$ , or  $\text{Ni}^{1+}$  configuration, while a photo-generated hole can move more or less itinerantly in the O  $2p$  valence band determining the hole-like photoconductivity [16].

Along with  $p$ - $d$  CT transitions an important contribution to the optical response of strongly correlated  $3d$  oxides can be related with strong dipole-allowed  $d$ - $d$  CT, or Mott transitions [6]. In NiO one expects a strong  $d$ - $d$  CT transition related with the  $\sigma$ - $\sigma$ -type  $e_g - e_g$  charge transfer  $t_{2g}^6 e_g^2 + t_{2g}^6 e_g^2 \rightarrow t_{2g}^6 e_g^3 + t_{2g}^6 e_g^1$  between  $nnn$  Ni sites with the creation of electron  $[\text{NiO}_6]^{11-}$  and hole  $[\text{NiO}_6]^{9-}$  centers (nominally  $\text{Ni}^{1+}$  and  $\text{Ni}^{3+}$  ions) thus forming a bound electron-hole dimer, or  $d$ - $d$  CT exciton. The charge, spin, and orbital degeneracy of the final state of this unique anti-Jahn–Teller transition  ${}^3A_{2g} + {}^3A_{2g} \rightarrow {}^2E_g + {}^2E_g$  gives rise to its complex structure. Thus the exchange tunnel reaction  $\text{Ni}^{1+} + \text{Ni}^{3+} \leftrightarrow \text{Ni}^{3+} + \text{Ni}^{1+}$  due to a two-electron transfer gives rise to two symmetric ( $S$ - and  $P$ -) excitons (see

Fig. 2) having  $s$ - and  $p$ -symmetry, respectively, with energy separation  $\delta_0 = 2|t|$  and  $\delta_1 = \frac{2}{3}|t|$  for the spin

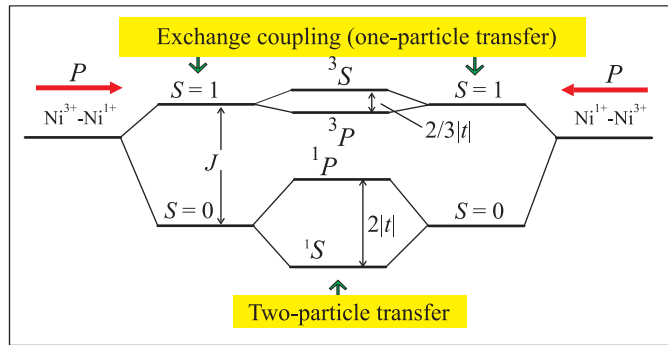


Fig. 2. (Color online) Illustration to formation of spin singlet and spin triplet  $S$ - and  $P$ -type  $d$ - $d$  CT excitons in NiO

singlet and spin triplet excitons, where  $t$  is the two-electron transfer integral which magnitude is of the order of  $\text{Ni}^{2+} - \text{Ni}^{2+}$  exchange integral [17]. Interestingly that  $P$ -exciton is dipole-allowed while  $S$ -exciton is dipole-forbidden. Strong dipole-allowed Franck–Condon  $d(e_g) - d(e_g)$  CT transition in NiO manifests itself as a strong spectral feature near 4.5 eV clearly visible in the absorption of thin NiO films [18], RIXS spectra [8, 9], the reflectance spectra (4.3 eV) [10]. Such a strong absorption near 4.5 eV is beyond the predictions of the  $p$ - $d$  CT model and indeed is lacking in absorption spectra of MgO:Ni [11]. It should be noted that, unlike all the above mentioned structureless spectra, the nonlinear absorption spectra [13] of NiO films do reveal anticipated “fine” structure with two narrow peaks at 4.075 and 4.33 eV preceding strong absorption above 4.575 eV. Interestingly that the separation 0.2–0.3 eV between the peaks is typical for exchange induced splittings in NiO (see, e.g., the “0.24 eV” optical feature [7]).

**Photoluminescence of NiO.** Although the optical absorption of NiO have been studied experimentally with some detail, their optical emission properties have been scarcely investigated.

Measurements performed with UV excitation below and near optical gap [14, 19, 20] point to a broad luminescence band in the region 2–3.5 eV. The observed emission bands in the visible and near infrared spectral ranges are usually attributed to  $\text{Ni}^{2+}$  intrasite, or crystal field  $d$ - $d$  transitions. In particular, the main green luminescence band peaked near 2.3 eV is attributed to a Stokes-shifted  ${}^1T_{2g}(D) \rightarrow {}^3A_{2g}(F)$  transition while the low-energy band peaked near 1.5 eV is related to  ${}^1E_g(D) \rightarrow {}^3A_{2g}(F)$  transition [21] (see Fig. 1 for the spectrum of the crystal field  $d$ - $d$  transitions [7]). However, the photoluminescence spectra of bulk single crystals

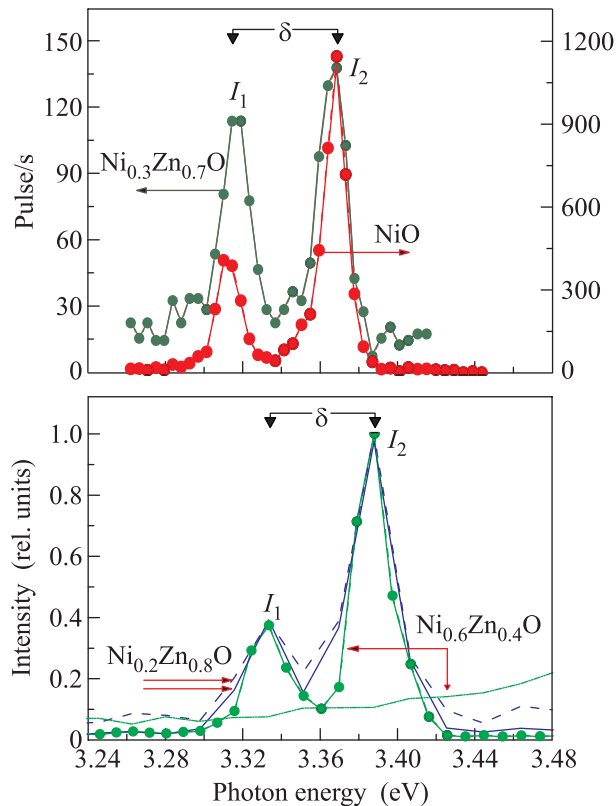


Fig. 3. (Color online) XUV excited luminescence spectra of NiO and solid solutions  $\text{Ni}_x\text{Zn}_{1-x}\text{O}$  (fast window, spectral resolution 10 meV). Upper panel: Luminescence spectra of the cellulose coated NiO and  $\text{Ni}_{0.3}\text{Zn}_{0.7}\text{O}$  samples under XUV excitation with energy  $E_{\text{exc}} = 130$  eV at  $T = 7.2$  K. Bottom panel: Low-temperature ( $T = 7.5$  K) luminescence spectra of the  $\text{Ni}_{0.2}\text{Zn}_{0.8}\text{O}$  and  $\text{Ni}_{0.6}\text{Zn}_{0.4}\text{O}$  cellulose free samples under XUV excitation with energy  $E_{\text{exc}} = 130$  eV (solid line) and  $E_{\text{exc}} = 450$  eV (dashed line). Luminescence spectra of  $\text{Ni}_{0.6}\text{Zn}_{0.4}\text{O}$  under XUV excitation with energy  $E_{\text{exc}} = 130$  eV at  $T = 7.2$  K (solid line) and room temperature (dash-and-dotted line)

and ceramics of NiO under 3.81 eV photoexcitation [20] suggestive the band gap excitation have revealed in addition to the green band a more intensive broad violet PL band with a maximum around 3 eV. The band was related to a  $p$ - $d$  charge transfer. Radiative recombination of carriers in powdered pellets of NiO under UV excitation with  $E_{\text{exc}} = 4.43$  eV (280 nm) higher than the CT gap consists at 10 K of a broad intensive band peaked at 2.8 eV with a shoulder centered at about 3.2 eV [19]. Furthermore, the 3.2 eV band reveals a two-peak structure clearly visible at elevated temperatures. Different kinetic properties, seemingly different temperature behavior [19] point to different relaxation channels governing the green and violet luminescence.

It is worth noting that all the studies of the PL in NiO point to a special role of different defects and the surface induced local non-cubic distortions in photoemission enhancement and a remarkable inhomogeneous broadening of the PL bands. Indeed, a most effective absorption of photons with the energy  $\hbar\omega \geq E_g$  in NiO given absorption coefficient  $\geq 5 \cdot 10^5 \text{ cm}^{-1}$  (Ref. [7]) occurs in a thin (10–20 nm) surface layer with more or less distorted symmetry and enhanced defect concentration. In other words, the UV photoexcitation cannot stimulate the bulk luminescence mirroring the fundamental material properties. These issues did motivate our studies of the photoluminescence spectra in NiO under high-energy soft X-ray time-resolved PL excitation technique.

**X-ray excited luminescence of NiO: experimental results.** The PL measurements were made on the samples of NiO and several solid solutions  $\text{Ni}_x\text{Zn}_{1-x}\text{O}$  ( $x = 0.2, 0.3,$  and  $0.6$ ) with the rocksalt-type crystal structure. As starting material we have used the commercially available powder of NiO (99%; Prolabo) and ZnO (99.99%; Alfa Aesar) which has been pressed into pellets under pressure of about 1250 bar and placed into gold capsules. Quenching experiments at 7.7 GPa and 1000–1100 K have been performed using a toroid-type high-pressure apparatus. Details of experimental technique and calibration are described elsewhere [22]. Electron microscopy analysis shows the samples to be dense poreless oxide ceramics with rock salt cubic structure and grain size of about 10–20  $\mu\text{m}$ . The NiO and  $\text{Ni}_{0.3}\text{Zn}_{0.7}\text{O}$  ceramic samples have been grinded with cellulose (carboxymethylcellulose, CMC) and then pressed into tablets to provide an enhancement of the luminescence intensity due to the effective surface enlargement [23].

The measurements of PL spectra under soft X-ray (XUV) excitation were made on a SUPERLUMI station (HASYLAB (DESY), Hamburg) using an ARC Spectra Pro-308i monochromator and R6358P Hamamatsu photomultiplier. The time-resolved PL spectra as well as the PL decay kinetics under XUV excitation has been measured on a BW3 beamline by a VUV monochromator (Seya–Namioka scheme) equipped with microchannel plate-photomultiplier (MCP 1645, Hamamatsu). The parameters of time windows:  $\delta t = 0.1$  ns,  $\Delta t = 5.7$  ns. The temporal resolution of the whole detection system was 250 ps. The temporary interval between SR excitation pulses is equal 96 ns.

Luminescence spectra of NiO under XUV excitation with energy  $E_{\text{exc}} = 130$  eV and fast window opening by 100 ps after the excitation impulse start are presented in Fig. 3. The XUV excited luminescence reveals puzzling spectral features with two close and very narrow lines

$I_1$  and  $I_2$  with a short decay-time  $\tau < 400$  ps peaked for NiO sample at 3.310 eV (linewidth 17 meV) and 3.369 eV (linewidth 13 meV), respectively, mounted on a weak broad structureless pedestal in the 2.5–4 eV range which is actually observed only for slow window. It is worth noting that different optical reflectance and absorption measurements [7, 10, 24] did not reveal the  $I_1$ - $I_2$  doublet.

To the best of our knowledge, such an unusual luminescence has not been observed to date either in NiO or other  $3d$  oxides. From the other hand, the well isolated  $I_1$ - $I_2$  doublet in the XUV excited luminescence seems to be a close relative of the broad high-energy (violet) band in PL spectra peaked near 3.2 eV. Dramatic difference in violet luminescence spectra under XUV and VUV excitation can be explained if to account for different penetration depth of VUV and XUV quanta. XUV excitation stimulates the bulk luminescence mirroring the fundamental material properties while the UV photoexcitation stimulates thin surface layers which irregularities give rise to a strongly enhanced and inhomogeneously broadened luminescence. To examine the origin of the unconventional  $I_1$ - $I_2$  doublet and make more reasonable suggestions about its nature we have made the measurements of the XUV excited luminescence for solid solution  $\text{Ni}_{0.3}\text{Zn}_{0.7}\text{O}$ . As in NiO we observed the  $I_1$ - $I_2$  doublet actually with the same energies and close linewidths. However, the integral intensity of the  $I_1$ - $I_2$  doublet in  $\text{Ni}_{0.3}\text{Zn}_{0.7}\text{O}$  is appeared to be almost ten times weaker than in NiO that points to the relation of the  $I_1$ - $I_2$  doublet with an emission produced by somehow coupled pairs of Ni ions. To exclude conceivable parasitic effect of the cellulose coating we have made the measurements of the XUV excited luminescence for cellulose free ceramic samples of solid solutions  $\text{Ni}_{0.2}\text{Zn}_{0.8}\text{O}$  and  $\text{Ni}_{0.6}\text{Zn}_{0.4}\text{O}$  (Fig. 3, bottom panel). For the both samples we have observed the same  $I_1$ - $I_2$  doublet structure of the luminescence spectra with practically the same energy separation  $\delta \approx 60$  meV and a small 20 meV blue shift as compared with NiO and  $\text{Ni}_{0.3}\text{Zn}_{0.7}\text{O}$  samples. Such a shift is believed to arise from small strains induced by coatings. Interestingly, the novel luminescence is clearly visible only at low temperatures: room temperature measurements do not reveal noticeable effect (see RT spectrum for  $\text{Ni}_{0.6}\text{Zn}_{0.4}\text{O}$  in Fig. 3 typical for other samples). As it is seen in Fig. 3 (bottom panel) the XUV excitation with higher energy  $E_{\text{exc}} = 450$  eV does induce nearly the same  $I_1$ - $I_2$  doublet structure of the luminescence spectra.

**Discussion.** What is the origin of the unconventional  $X$ -ray excited luminescence? There are three types of candidate initial states for the radiative transition: 1) excited  ${}^1T_{1g}(G)$  or  ${}^1A_{1g}(G)$  terms of  $\text{Ni}^{2+}3d^8$

configuration which Franck-Condon energies are found by Newman and Chrenko [7] as 3.52 and 3.25 eV, respectively; 2) self-trapped  $p$ - $d$  ( $t_{1g}(\pi) \rightarrow e_g$ ) CT exciton, 3) self-trapped  $d$ - $d$  ( $e_g \rightarrow e_g$ ) CT exciton.

Several arguments rule out the  $d$ - $d$  crystal field transitions  ${}^1T_{1g}(G)$ ,  ${}^1A_{1g}(G) \rightarrow {}^3A_{2g}(F)$  as a source of unconventional  $X$ -ray excited luminescence. First, the excited  ${}^1T_{1g}(G)$  and  ${}^1A_{1g}(G)$  terms can non-radiatively relax to close low-lying terms  ${}^3T_{1g}(P)$  and  ${}^1T_{2g}(D)$ . Second, typically the radiative crystal field transitions produce broad luminescence bands with long lifetimes [19]. Third, the energies of the  $d$ - $d$  crystal field transitions are expected to strongly depend on the Ni concentration in  $\text{Ni}_x\text{Zn}_{1-x}\text{O}$ , whereas the energy of the  $I_1$ - $I_2$  doublet hardly if any depends on  $x$ .

However, the low-lying  $p$ - $d$  ( $t_{1g}(\pi) \rightarrow e_g$ ) CT excitonic states are also unlikely responsible for the violet luminescence in NiO. Indeed, instead of the rather weak  $p$ - $d$  CT excitation channel of the  $\pi \rightarrow \sigma$  type the most effective channel of the recombinational relaxation for the spin-triplet  $p$ - $d$  CT states  $t_{2g}^6 e_g^3 \gamma(\pi)$  ( $\gamma(\pi) = t_{1g}(\pi), t_{2u}(\pi), t_{1u}(\pi)$ ) in NiO implies the stronger  $\pi \rightarrow \pi$  transfer  $t_{2g} \rightarrow \gamma(\pi)$  with formation of excited spin-triplet  ${}^3T_{1g}$  or  ${}^3T_{2g}$  states of the  $t_{2g}^5 e_g^3$  configuration of  $\text{Ni}^{2+}$  ion followed by final relaxation to lowest singlet terms  ${}^1T_{2g}$  and  ${}^1E_g$  producing green and red luminescence, respectively. Obviously, this relaxation is strongly enhanced by any symmetry breaking effects lifting or weakening the selection rules. It means the three  $\pi \rightarrow \sigma$   $p$ - $d$  CT transitions  $t_{1g}(\pi) \rightarrow e_g$ ,  $t_{2u}(\pi) \rightarrow e_g$ , and  $t_{1u}(\pi) \rightarrow e_g$  are expected to effectively stimulate the green luminescence in NiO, however, these  $p(\pi)$ - $d$  CT transitions cannot explain the origin of violet luminescence, in particular, specific  $I_1$ - $I_2$  doublet stimulated by XUV excitation which concentration behavior points to participation of Ni pairs, or  $d$ - $d$  CT transitions rather than isolated  $\text{NiO}_6$  centers.

It seems the unique “double” Jahn-Teller  $d$ - $d$  CT exciton  $t_{2g}^6 e_g^3; {}^2E_g + t_{2g}^6 e_g^1; {}^2E_g$  self-trapped in the lattice due to electron-hole attraction and strong Jahn-Teller coupling with a reasonable Stokes shift of  $\sim 1$  eV remains to be the only candidate to produce unconventional  $X$ -ray excited luminescence. In such a case the  $I_1$ - $I_2$  doublet can be a Stokes shifted radiative counterpart of  $X_1$ - $X_2$  (or  $X_2$ - $X_3$ ) excitonic states observed in nonlinear optical absorption spectra of NiO films [13] (see Fig. 2). More explicit assignment of  $I_1$  and  $I_2$  lines requires further detailed analysis of electron-lattice, spin-orbital, and exchange coupling effects together with additional measurements of temperature and external field effects. Narrowness of the  $I_1$  and  $I_2$  lines underlines an

extremely localized character of the double Jahn–Teller  $d$ - $d$  CT exciton.

Temperature quenching of the  $I_1$ - $I_2$  luminescence can be explained by the nonradiative transition to a nearby  $d$ - $d$  CT excitonic state  $t_{2g}^6 e_g^3; {}^2E_g + t_{2g}^5 e_g^2; {}^4T_{1g}$ . Indeed, given  $Dq \approx 0.1$  eV [7] the  $t_{2g}^6 e_g^1; {}^2E_g$  state is an excited state of  $\text{Ni}^{3+}$  ion that is separated from the true ground state  $t_{2g}^5 e_g^2; {}^4T_{1g}$  by the gap of  $\sim 1.0$  eV. It should be noted, however, that the transformation  $t_{2g}^6 e_g^1; {}^2E_g \rightarrow t_{2g}^5 e_g^2; {}^4T_{1g}$  of  $\text{Ni}^{3+}$  center implies the configurational change that strongly suppress its probability. The self-trapped  $t_{2g}^6 e_g^3; {}^2E_g + t_{2g}^5 e_g^2; {}^4T_{1g}$  exciton, in turn, has an effective radiation channel due to  $\sigma \rightarrow \sigma$   $d$ - $d$  CT recombination transition to  $t_{2g}^6 e_g^2; {}^3A_{2g} + t_{2g}^5 e_g^3; {}^3T_{2g}$  state which corresponds to  $\text{Ni}^{2+}$ - $\text{Ni}^{2+}$  configuration with one of ions in the excited  $t_{2g}^5 e_g^3; {}^3T_{2g}$  state. In other words, the temperature quenching of the  $I_1$ - $I_2$  luminescence can be accompanied with the ignition of the luminescence in the spectral range 1–2 eV.

It is worth noting that self-trapped  $d$ - $d$  excitons can be formed also due to a trapping of the oxygen hole borned by the  $p$ - $d$  CT transition on the nearest  $\text{Ni}^{2+}$  ion. Furthermore, the excitation of the  $t_{2g}^6 e_g^3 t_{1g}(\pi)$   $p$ - $d$  CT exciton at energy 3.7 eV that is sizeably below the energy of the strongest  $d$ - $d$  CT transition at 4.5 eV can efficiently stimulate the unconventional  $I_1$ - $I_2$  luminescence due to a self-trapping of the oxygen  $t_{1g}(\pi)$ -hole in the  $t_{2g}$  orbital on the adjacent  $\text{Ni}^{2+}$  ion.

**Conclusion.** Luminescence spectra of NiO and solid solutions  $\text{Ni}_x\text{Zn}_{1-x}\text{O}$  with the rocksalt-type structure have been investigated under XUV excitation with two excitation energy, 130 and 450 eV. Soft  $X$ -ray excitation makes it possible to avoid the predominant role of the surface effects in luminescence and reveal bulk luminescence with puzzling well isolated  $I_1$ - $I_2$  doublet of very narrow lines with close energies near 3.3 eV in both NiO and solid solutions  $\text{Ni}_x\text{Zn}_{1-x}\text{O}$ . Comparative analysis of the  $p$ - $d$  and  $d$ - $d$  CT transitions, their relaxation channels, and luminescence spectra for NiO and  $\text{Ni}_{0.3}\text{Zn}_{0.7}\text{O}$  points to recombination radiative transition in self-trapped  $nnn$   $\text{Ni}^+-\text{Ni}^{3+}$   $d$ - $d$  CT excitons as the only candidate source of unconventional luminescence. To the best of our knowledge it is the first observation of the self-trapping and luminescence for  $d$ - $d$  CT excitons.

The authors are grateful to R.V. Pisarev for helpful discussions. This work was partially supported by the Ural Branch of RAS (Grant # 12-U-2-1030) and RFBR Grants # 10-02-96032 and 12-02-01039 (A.S.M.).

1. K. S. Song and R. T. Williams, *Self-Trapped Excitons*, Springer-Verlag, Berlin, 1993.
2. V. I. Sokolov and K. A. Kikoin, *Sov. Sci. Rev. A* **12**, 147 (1989); V. I. Sokolov, *Semiconductors* **28**, 329 (1994).
3. R. Dingle, *Phys. Rev. Lett.* **23**, 579 (1969); D. J. Robbins, *J. Lumin.* **24/25**, 137 (1981).
4. L. van Pieterse, M. Heeroma, E. de Heer, and A. Meijerink, *J. Lumin.* **91**, 177 (2000).
5. B. Brandow, *Adv. Phys.* **26**, 651 (1977); S. Hüfner, *Adv. Phys.* **43**, 183 (1994).
6. A. S. Moskvina, *Phys. Rev. B* **65**, 205113 (2002); R. V. Pisarev, A. S. Moskvina, A. M. Kalashnikova, and Th. Rasing, *Phys. Rev. B* **79**, 235128 (2009); A. S. Moskvina and R. V. Pisarev, *Low Temp. Phys.* **36**, 613 (2010); A. S. Moskvina, *Optics and Spectroscopy*, **111**, 403 (2011).
7. R. Newman and R. M. Chrenko, *Phys. Rev.* **114**, 1507 (1959).
8. N. Hiraoka, H. Okamura, H. Ishii et al., *Eur. Phys. J. B* **70**, 157 (2009).
9. L.-C. Duda, T. Schmitt, M. Magnuson et al., *Phys. Rev. Lett.* **96**, 067402 (2006).
10. R. J. Powell and W. E. Spicer, *Phys. Rev. B* **2**, 2182 (1970).
11. K. W. Blazey, *Physica B* **89**, 47 (1977).
12. J. L. McNatt, *Phys. Rev. Lett.* **23**, 915 (1969); R. Glosser and W. C. Walker, *Solid State Commun* **9**, 1599 (1971).
13. S. I. Shablaev and R. V. Pisarev, *Physics of the Solid State* **45**, 1742 (2003).
14. V. V. Volkov, Z. L. Wang, and B. S. Zou, *Chemical Phys. Lett.* **337**, 117 (2001).
15. S. Chakrabarty and K. Chatterjee, *Journal of Physical Sciences* **13**, 245 (2009).
16. Ja. M. Ksendzov and I. A. Drabkin, *Sov. Phys. Solid State* **7**, 1519 (1965).
17. A. S. Moskvina, *Phys. Rev. B* **84**, 075116 (2011).
18. C. E. Rossi and W. Paul, *J. Phys. Chem. Solids* **30**, 2295 (1969).
19. C. Díaz-Guerra, A. Remón, J. A. García, and J. Piqueras, *Phys. Stat. Solidi (a)* **163**, 497 (1997).
20. S. Mochizuki and T. Saito, *Physica B* **404**, 4850 (2009).
21. A. Kuzmin, N. Mironova-Ulmane, and S. Rochin, *Proceedings SPIE* **5122**, 61 (2003).
22. A. N. Baranov, P. S. Sokolov, O. O. Kurakevich et al., *High Pressure Research* **28**, 515 (2008).
23. Actually the cellulose coating yielded a two-threefold magnification of the PL intensity.
24. V. Propach, D. Reinen, H. Drenkhahn, and H. Müller-Buschlaum, *Z. Naturforsch. B* **33**, 619 (1978).